Mutation of Y407 in the CH3 domain dramatically alters glycosylation and structure of human IgG

Rebecca J. Rose,[1,2,†] Patrick H.C. van Berkel,[3,†] Ewald T.J. van den Bremer,[3] Aran F. Labrijn,[3] Tom Vink,[3] Janine Schuurman,[3] Albert J.R. Heck[1,2,*] and Paul W.H.I. Parren[3]

[1]Biomolecular Mass Spectrometry and Proteomics Group; Bijvoet Center for Biomolecular Research and Utrecht Institute for Pharmaceutical Sciences; Utrecht University; Utrecht, The Netherlands; [2]Netherlands Proteomics Centre; Utrecht, The Netherlands; [3]Genmab; Utrecht, The Netherlands

[†]These authors contributed equally to this work.

Keywords: N-linked glycosylation, sialic acid, antibody structure, hydrogen-deuterium exchange, native mass spectrometry

Antibody engineering is increasingly being used to influence the properties of monoclonal antibodies to improve their biotherapeutic potential. One important aspect of this is the modulation of glycosylation as a strategy to improve efficacy. Here, we describe mutations of Y407 in the CH3 domain of IgG1 and IgG4 that significantly increase sialylation, galactosylation, and branching of the N-linked glycans in the CH2 domain. These mutations also promote the formation of monomeric assemblies (one heavy-light chain pair). Hydrogen-deuterium exchange mass spectrometry was used to probe conformational changes in IgG1-Y407E, revealing, as expected, a more exposed CH3-CH3 dimerization interface. Additionally, allosteric structural effects in the CH2 domain and in the CH2-CH3 interface were identified, providing a possible explanation for the dramatic change in glycosylation. Thus, the mutation of Y407 in the CH3 domain remarkably affects both antibody conformation and glycosylation, which not only alters our understanding of antibody structure, but also reveals possibilities for obtaining recombinant IgG with glycosylation tailored for clinical applications.

Introduction

Human IgG is a protein of ~150 kDa, consisting of two heavy (H)-light (L) chain pairs of about 75,000 Da each. An IgG contains two Fab regions that bind antigens and an Fc region that mediates immune effector functions and is involved in homeostasis of the protein. Each Fab is formed by part of the heavy chain (VH and CH1) covalently linked to the whole light chain, whereas the Fc part is formed by dimerization of the CH2 and CH3 domains of each heavy chain. The IgG Fc contains two N-linked glycans, one on each heavy chain at position N297 in the CH2 domain.[1] The first steps of N-linked glycosylation occur in the endoplasmic reticulum (ER) during mRNA translation.[2] Further modification occurs in the ER, yielding oligomannose glycans that can be matured further in the Golgi, yielding hybrid and complex type glycans[2] with different degrees of branching (i.e., bi, tri or tetra-antennary). In the case of human IgG, the majority of N-linked glycans is of the complex biantennary type lacking the terminal galactose or sialic acid.

Since the mid-1990s, antibodies have become an important class of drugs, with more than 28 antibodies approved for therapeutic use in the US and Europe.[3] Initially, these approved antibodies were based on mouse IgG or chimeric IgG; more recently, antibodies based on humanized or fully human IgG sequences have entered the market. The search for strategies to improve clinical efficacy of antibodies further is continuously ongoing. This research is also fuelled by the growing understanding of both the underlying mechanisms and the current limitations of antibody-based treatment. Engineering of antibodies has enabled the design of antibody-based formats with tailored pharmacokinetics, avidity, (bi-)specificity and increased tumor penetration.[3] Modification of the N-linked glycosylation of monoclonal antibodies (mAbs) has also received interest as a strategy for improving the efficacy of therapeutic antibodies. For instance, galactose and fucose play a distinct role in complement-dependent cytotoxicity (CDC)[4-6] and antibody-dependent cell- mediated cytotoxicity (ADCC),[7,8] respectively. It was recently shown that the anti-inflammatory activity of IgG can be explained by the presence of α(2,6)-sialylated N-linked glycans in the Fc.[9-12] Another option for improving the efficacy of therapeutic mAbs is engineering of the Fc protein backbone in such a way that the interaction with complement or IgG Fc receptors is optimized.[13]

Here, we describe a 'monomeric' human IgG format (i.e., existing predominantly as a single heavy chain-light chain pair (HL) as opposed to the typical intact (HL)$_2$ structure) with a radically different N-linked glycosylation profile, based on mutation of the Y407 residue in the CH3 domain. Uniquely, these Y407 variants can contain N-linked glycans with increased galactose and sialic acids and, depending on the host cell, show considerably increased branching. We show, using hydrogen-deuterium exchange mass spectrometry (HDX-MS),
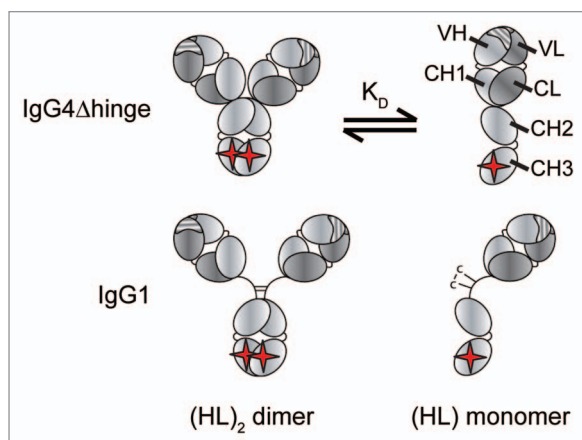
Figure 1. The structure of (top) IgG4Δhinge and (bottom) IgG1 monomer (HL) and dimer (HL)$_2$ used in this study. CH3 mutations are indicated with (red +).

that this dramatic change in glycosylation is likely due to significant structural changes occurring in the CH2 domain and the CH2-CH3 interface. These results together provide further insight into glycosylation of human IgG, as well as novel opportunities for the production of highly galactosylated and sialylated human IgG.

Results

Assembly and glycosylation of IgG4Δhinge Y407 variants. We previously reported a strategy for studying the CH3–CH3 interaction strength by introducing point-mutations in the CH3 domain of hinge-deleted IgG4 (further referred to as IgG4Δhinge, **Fig. 1**).[14] We identified a subset of CH3 mutations in IgG4Δhinge that resulted in significantly higher dissociation constants (K_Ds) of the CH3–CH3 interaction (ref. 14; a summary of the K_Ds is presented in **Table 1**). To analyze whether a weakened CH3–CH3 interaction affected the N-linked glycosylation of IgG4, high performance anion exchange chromatography with pulsed amperometric detection (HPAEC-PAD) was performed. The majority of CH3 mutants of IgG4Δhinge contained glycans similar to wild-type recombinant human IgG4 or IgG4Δhinge, i.e., mainly core-fucosylated complex bi-antennary type glycans lacking galactose and sialic acid (**Fig. 2A**; **Table 1**). A number of mutations, such as IgG4Δhinge-L368V, -L368T, -E357V, -F405R, -F405Q and S364R (**Table 1**), each with a weaker CH3–CH3 interaction compared with the wild-type (i.e., high K_D), resulted in glycans with slightly higher galactosylation or increased amount of tri-antennary structures; however, sialylation of these mutants remained low. Interestingly, four mutations, IgG4Δhinge-Y407A, -Y407Q, -Y407K, -Y407E, each with a high K_D, clearly showed dramatically increased galactosylation, branching and sialylation; even tri-antennary sialylated structures were identified. As an example, the HPAEC-PAD profile of IgG4Δhinge-Y407E, compared with the wild-type equivalent and a mutation with a regular glycosylation pattern, is shown in **Figure 2**.

Double mutants of IgG4Δhinge were generated to disrupt the CH3–CH3 interface further. The combination of mutation at position 407 with the mutation of another residue, such as D399 or F405, further increased the K_D, but abrogated the effect observed in the single Y407 mutants with respect to sialylation or branching. As a result, the glycosylation profile was closer to wild type IgG (**Table 1B**). For all mutants, core-fucosylation levels were comparable to those obtained for IgG4 or IgG4Δhinge.

Assembly and glycosylation of IgG1 Y407 variants. IgG4 molecules are characterized by a hinge region that forms both inter-heavy chain and intra-heavy chain disulfide bonds. This characteristic, in combination with their relatively weak inter-chain CH3 domain interaction (relative to IgG1), makes IgG4 molecules unstable in vivo.[15] This behavior is significantly enhanced in the hinge-deleted constructs, and further manipulated with mutations in the CH3 domain, as described above. We next studied the effects of mutating amino acid Y407 on monomer formation and glycosylation in IgG1 molecules (**Fig. 1**). Two mutants, IgG1-Y407E and IgG1-Y407A, were transiently expressed in HEK-293F or CHO-S cells, purified and characterized using SDS-PAGE, native ESI-MS, HP-SEC and HPAEC-PAD. IgG1-Y407A was found to populate the intact 'dimeric' (HL)$_2$ state, with a molecular weight of approximately 150 kDa (**Fig. 3A**). In contrast, however, IgG1-Y407E was predominantly monomeric HL, with a molecular weight of ~75 kDa (**Fig. 3A**). A minor species at 150 kDa was also observed by non-reducing SDS-PAGE, indicating a minor population of covalently bound (HL)$_2$. Native MS analysis confirmed that IgG1-Y407E indeed forms very little non-covalently bound dimer and mainly populates a monomeric state under non-denaturing conditions (**Fig. 3B**).

The glycosylation profile of IgG1-Y407E is shown in **Figure 4**, in comparison to recombinant wild-type human IgG1, and summarized in **Table 2**. In agreement with the IgG4 Y407 mutants, IgG1-Y407E also contained higher levels of galactose and sialic acid, when produced in both HEK-293F cells (**Fig. 4B**; **Fig. S2**) and CHO-S (**Fig. 4C**; **Fig. S2**). Glycosylation of IgG1-Y407E produced in HEK-293F, however, was substantially more heterogeneous compared with that produced in CHO-S. First, IgG1-Y407E produced in HEK-293F contained both α(2,3) and α(2,6) linked N-acetylneuraminic acid, whereas IgG1-Y407E from CHO-S contained only α(2,3) linked N-acetylneuraminic acid (**Fig. S4**). Second, IgG1-Y407E from HEK-293F also contained more tri-antennary structures compared with the mutant produced in CHO-S (**Table 2**). The glycosylation profile of IgG1-Y407A produced in both cell lines was comparable to wild-type recombinant human IgG1 (**Table 2**).

Relationship between glycosylation and oligomerization state. Clearly, the N-linked glycosylation of IgG1-Y407E differs significantly compared with IgG1-Y407A and wild-type human IgG1, while IgG1-Y407E also contains much more monomeric HL. To determine whether monomericity is a prerequisite for changes in glycosylation, the monomeric HL and dimeric (HL)$_2$ portions of IgG1-Y407E were fractionated by preparative SEC. The N-linked glycosylation of HL and (HL)$_2$ was highly comparable, i.e., the dimeric (HL)$_2$ fraction contained similar levels of

Table 1. Summary of the N-linked glycosylation analyses of IgG4Δhinge mutants with a single mutation (A) or double mutation (B)

Table 1A Protein	K_D (µM)	Glycan structure (% of total)							
		G0F	G1F	G2F	Bi	Tri	1SA	2SA	3SA
IgG4 (*wt*)	-	42	34	10	87	13	1	-	-
IgG4-Δhinge (*wt*)	0.0495	34	29	13	84	16	2	-	-
IgG4-Δhinge-*mutation*									
-R409K	0.0004	36	29	13	84	16	3	-	-
-K370A	0.0017	44	28	10	91	9	2	-	-
-K370T	0.0021	45	29	10	91	9	1	-	-
-R409A	0.216	38	28	11	86	14	2	-	-
-D399S	6.46	37	32	12	82	18	2	-	-
-L368A	7.64	37	33	12	84	16	2	-	-
-L368E	10.7	48	26	7	89	11	2	-	-
-L368V	**11.4**	**24**	**33**	**21**	**79**	**21**	**4**	**-**	**-**
-L368S	11.7	42	33	11	86	14	2	-	-
-T366A	14.9	32	30	16	82	18	3	-	-
-D399A	22.2	41	31	12	87	13	2	-	-
-F405A	22.5	33	30	14	80	20	2	-	-
-F405L	26.7	37	30	12	84	16	2	-	-
-F405Y	36.6	37	35	14	83	17	2	-	-
-L368T	**42.3**	**40**	**35**	**11**	**77**	**23**	**2**	**-**	**-**
-E357A	59.2	33	32	17	85	15	4	-	-
-E357V	**62.6**	**25**	**34**	**21**	**84**	**16**	**4**	**-**	**-**
-F405D	65.8	41	31	11	85	15	3	-	-
-L368G	69.6	44	30	10	87	13	2	-	-
-Y407A	**71.6**	**21**	**23**	**21**	**74**	**26**	**8**	**4**	**-**
-F405T	85.1	43	30	10	85	15	2	-	-
-Y407Q	**96.8**	**4**	**7**	**18**	**52**	**48**	**27**	**21**	**2**
-Y407K	**97.0**	**10**	**17**	**24**	**66**	**34**	**17**	**11**	**-**
-Y407E	**107.8**	**5**	**7**	**17**	**52**	**48**	**25**	**25**	**3**
-S364R	**120.0**	**17**	**28**	**24**	**71**	**29**	**9**	**2**	**-**
-F405R	**164.7**	**24**	**34**	**19**	**75**	**25**	**5**	**-**	**-**
-F405Q	**190.7**	**25**	**34**	**20**	**77**	**23**	**5**	**-**	**-**
Table 1B Protein	K_D (µM)	Glycan structure (% of total)							
		G0F	G1F	G2F	Bi	Tri	1SA	2SA	3SA
IgG4 (*wt*)	-	42	34	10	87	13	1	-	-
IgG4-Δhinge (*wt*)	0.0495	34	29	13	84	16	2	-	-
IgG4-Δhinge-*mutation*									
-D399S/Y407E	87.5	24	32	20	75	25	5	-	-
-D399S/Y407K	109.4	25	32	18	73	27	5	-	-
-D399S/Y407Q	120.2	25	33	18	74	26	5	-	-
-F405D/Y407E	143.3	32	33	15	83	17	6	-	-
-F405T/Y407E	147.9	34	33	15	81	19	4	-	-

The N-linked glycan profiles were determined by HPAEC-PAD. KD values were determined previously by MS.[14] All proteins were expressed in HEK-293F cells.
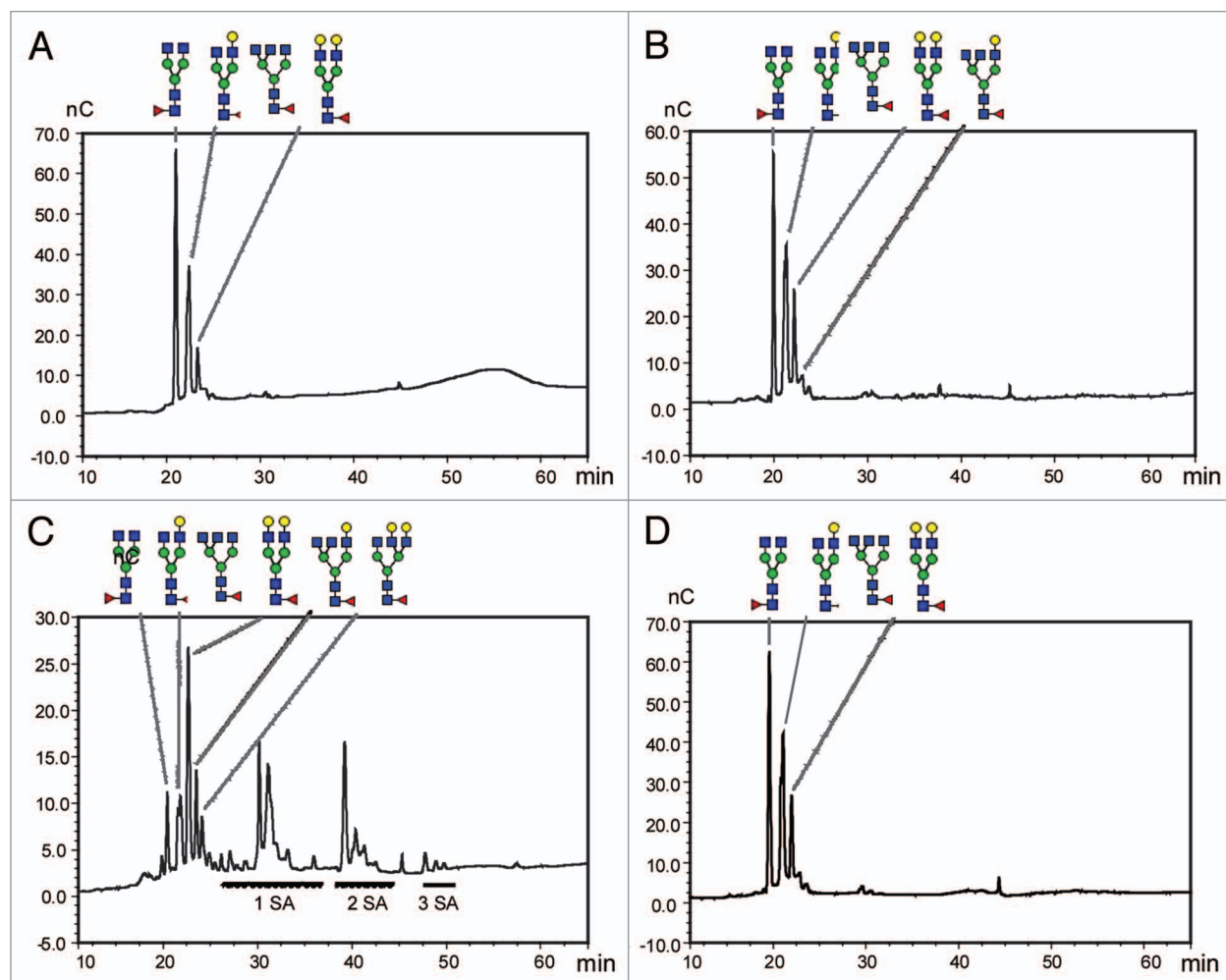
Figure 2. HPAEC-PAD analysis of N-linked glycosylation of (**A**) IgG4, (**B**) IgG4Δhinge, (**C**) IgG4Δhinge-Y407E and (**D**) IgG4Δhinge-T366A. IgG4Δhinge-T366A is an example where the glycosylation is highly comparable to wild type IgG4 and IgG4Δhinge. Glycan structures are explained in **Figure S1**.

galactose, sialic acid and branching compared with that observed in the monomeric HL fraction (**Fig. 4C and D**).

To test further whether monomericity is important for the extended N-linked glycosylation observed, the three mutations that weakened CH3–CH3 interactions in IgG4Δhinge most severely (i.e., S364R, F405T/Y407E and F405Q, **Table 1**) were introduced in human IgG1. The mutants were expressed in HEK-293F cells. Each mutant contained a high percentage of monomer as evidenced by HP-SEC, SDS-PAGE and native MS, but the N-linked glycan profiles were comparable to wild-type IgG1 (**Fig. 3B**; **Table 2**). Hence, monomericity alone does not drive the maturation of the N-linked glycosylation.

The observed differences between Y407E and Y407A suggest that the nature of the residue at position 407 strongly affects both monomericity and glycosylation. Y407 was therefore substituted for every possible amino acid and in each case the abundance of monomeric HL was monitored in conjunction with the glycosylation profile. Although a number of mutations resulted in increased monomericity, only mutations to charged amino acids or glutamine affected glycosylation significantly, with smaller effects seen for Y407S, Y407G and Y407W (**Table S1**). Thus,

there is not a direct correlation between the monomeric population and extensive glycosylation, but rather, the glycosylation appears to be very sensitive to the chemical properties of the side-chain of the 407 residue.

Comparison with the F243A mutation. One other mutation, F243A, has previously been shown to affect glycosylation of IgG significantly.[16] We compared the glycosylation of IgG1-F243A with that of IgG1-Y407X and IgG1-F243A-Y407X (where X is D, E, R or K) expressed in HEK-293F cells. The F243A mutant indeed showed increased galactosylation and sialylation, in agreement with the previous study and also a substantially increased amount of tri-antennary structures (**Fig. S5**, blue curve). Compared with the glycosylation of IgG-Y407E (**Fig. S5**, red curve), the latter showed slightly lower galactosylation, but higher levels of sialylation and branching (**Table S2**). The effects of both mutations were not additive or synergistic as the F243A-Y407E mutant showed a glycan profile largely comparable to Y407E (**Fig. S5**, black curve; **Table S2**).

The glycan chains are covalently attached to the IgG structure at residue N297, on the interior of the CH2 domain, distal to the CH3 domain. Crystal structures of the IgG1 Fc region show that

F243 interacts directly with the glycan chain;[17-19] it is thought that eliminating this interaction in the F243A mutant destabilizes the nascent glycan chain. In contrast, the Y407 residue is located far away from N297 (~40 Å), in the CH3 domain, where it is buried in the interface between the two heavy chains. Thus, it is not apparent how the substitution of this side-chain has such a strong influence on the glycosylation. Having already ruled out a direct link between populating a monomeric state and the extended glycosylation, another explanation could be long-range structural effects of the mutation. To explore this possibility, we used hydrogen-deuterium exchange mass spectrometry (HDX-MS) to characterize the structure of IgG1-Y407E compared with wild-type IgG1. This technique measures the incorporation of deuterium as an indication of the structural/ dynamic exposure of different sites in a protein to the solvent. HDX-MS has previously been used to analyze structural changes of recombinant human IgG1 upon deglycosylation or methionine oxidation.[20-22]

Structural differences in IgG1 induced by Y407E mutation. To define conformational changes using HDX data, it is necessary to compare the protein in two difference states or with two potentially different structures. To probe differences between IgG1-Y407E and wild-type IgG1, the intact $(HL)_2$ dimer, purified by SEC, was used. First, both samples were enzymatically deglycosylated using PNGaseF, such that any differences observed must be due to inherent changes in the

Figure 3. (**A**) Non-reducing SDS-PAGE of IgG1-Y407E and IgG1-Y407A. Lane 1, IgG1 control from CHO-S; Lane 2, IgG1-Y407A from CHO-S; Lane 3, IgG1-Y407E from CHO-S; Lane 4, IgG1-Y407A from HEK-293F; Lane 5, IgG1-Y407E from HEK-293F. (**B**) Native MS analysis of wild-type IgG1, IgG1-Y407E, IgG1-F405T/Y407E, IgG1-S364R and IgG1-F405Q, purified from HEK-293F cells. The insets show enlarged spectra of single charge states, whereby the different peaks relate to the presence of different glycan chains. Note, IgG1-Y407A mass spectrum (not shown) is comparable to that of wild-type IgG1.

protein structure rather than interactions with the glycan chains. The deglycosylated proteins were incubated in D_2O for time intervals between 1 minute and 24 hours before the reaction was quenched. Subsequently, the protein was digested into peptides with an online peptic digestion followed by LC/MS analysis, allowing the relative deuterium incorporation to be determined for each peptide (see *Materials and Methods*). **Figure 5A** shows the difference in deuterium incorporation between wild-type IgG1 and the intact $(HL)_2$ dimer of IgG1-Y407E for representative peptides across the heavy chain sequence. Clearly, and as expected, there are no significant structural differences detected in the Fab regions of the IgG1. However, in the CH3 domain and also, remarkably, in much of the CH2 domain, Y407E shows significantly different HDX behavior compared with wild-type IgG1. This indicates that the mutation causes changes in structure (or dynamics) in both the CH2 and the CH3 domains. The main regions of change are represented on a crystal structure of the IgG1 Fc (PDB 1hzh; **Fig. 5B**). In the CH3–CH3 interface, the Y407E mutation caused higher deuterium uptake in peptides 349–364 and 391–398 (colored yellow in **Fig. 5B**), indicating that these structures are more exposed here. Structural changes in the CH2 domain indicated that several regions are less exposed or more rigid in Y407E (colored blue in **Fig. 5B**, peptides 235–241, 253–264, 307–318, 319–333). The loops and

helix forming the interface between the CH2 and CH3 domains are also less exposed to solvent in Y407E than in wild-type IgG1 (peptides 242–252 and 369–380). One region in the CH2, residues 300–306, shows higher exchange in Y407E. Changes in the structure in the CH2–CH3 interface and the CH2 domain could conceivably be responsible for affecting the heterogeneity of the glycan chains.

To probe whether the structural differences observed above are dependent on the glycosylation, HDX-MS analysis was next repeated using the glycosylated wild-type and IgG1-Y407E (**Fig. S7**). Again, significant increases in deuterium incorporation close to the CH3–CH3 interface were observed for the variant (colored yellow, peptides 349–358, 357–365, 391–398). An allosteric effect altering the structure of the CH2 domain is also observed (colored blue, peptides 287–306, 307–318); however, these changes are not identical to those in the deglycosylated counterparts. In particular the β-strand directly contacting the glycan chain (strand A, residues 239–243) shows no difference, suggesting that the glycan chains protect the protein structure from HDX equally in this region. Note that the peptides observed and measured for the glycosylated and deglycosylated samples were not identical, for example, cleavage at position 299/300 was much reduced in the glycosylated sample; presumably the protease cleavage site was sterically protected by

Table 2. Summary of the N-linked glycosylation analyses of IgG1 mutants

Protein	Host cell	% monomer	Glycan structure (% of total)							
			G0F	G1F	G2F	Bi	Tri	1SA	2SA	3SA
IgG1 (*wt*)	293F	0	41	27	7	90	10	2	-	-
IgG1-*Mutation*										
-Y407E	293F	90	5	9	16	49	51	29	20	2
-Y407E	CHO	95	12	9	14	86	14	17	30	3
-Y407A	293F	1	49	18	6	89	11	2	-	-
-Y407A	CHO	5	51	31	6	93	7	1	-	-
F405T/Y407E	293F	84	36	33	15	82	18	3	-	-
-F405Q	293F	48	45	28	11	84	16	2	-	-
-S364R	293F	43	41	29	12	84	16	4	-	-

The N-linked glycan profiles were determined by HPAEC-PAD. % monomer was calculated from HP-SEC data.
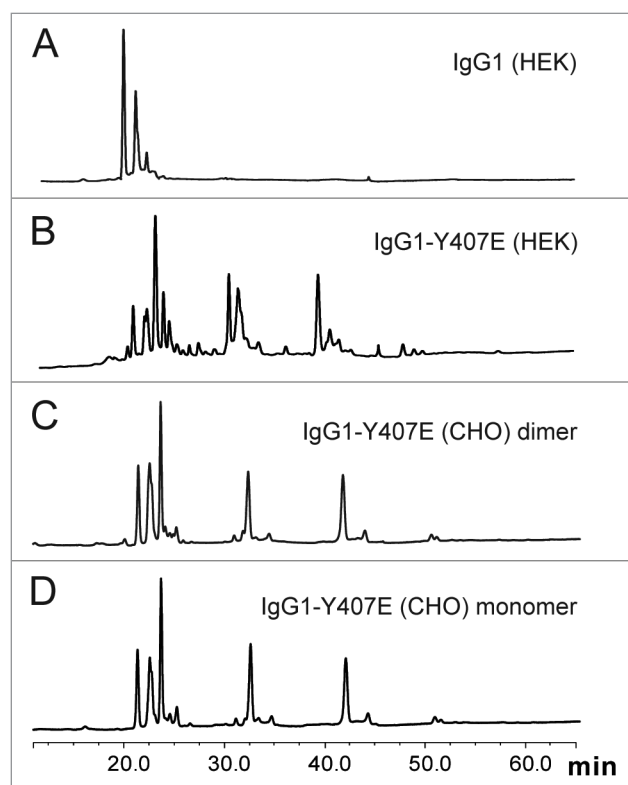
Figure 4. HPAEC-PAD traces of glycans of (**A**) IgG1, and IgG1-Y407E expressed in (**B**) HEK-293F or (**C and D**) CHO-S. The dimeric form (**C**) and monomeric form (**D**) of IgG1-Y407E expressed in CHO-S cells were purified by SEC before analysis. Y-axis shows intensity normalized to highest peak.

the glycans. Deuterium uptake plots for peptides throughout the heavy chain sequence, from both deglycosylated and glycosylated samples, are given in **Figure S8**.

Deconvolving structural effects of monomericity from Y407E mutation. IgG1-Y407E has a propensity to exist as monomeric (HL), and indeed the HDX-MS results from the covalently-bound (HL)$_2$ presented above revealed the structural basis for this: the CH3 interface is much more exposed to solvent, implying a weaker interaction here. To differentiate the effects on monomer/dimer propensity of the Y407E mutation from the effects on glycosylation, HDX-MS data were subsequently collected to compare the IgG1-Y407E HL construct with the double mutant IgG1-F405T/Y407E, which also populates the HL monomeric state, but with a wild-type IgG-like glycan profile (**Table 1**; **Fig. 3B**). Both glycosylated and enzymatically deglycosylated samples were analyzed (summary of the data for deglycosylated samples are shown in **Fig. S9**; uptake graphs for all samples are given in **Fig. S10**). Conformational differences between the Y407E monomer and the double mutant control were again observed in the CH2 and CH3 domains, as in the (HL)$_2$ dimer. Fewer significant regions of change were observed in the monomer CH2 domain; note also that peptide 253–264 could not be quantified accurately in these samples, so no data are known for this region. These data indicate that some changes in the CH2 domain may be connected to the Y407 to E mutation itself or the resulting monomeric propensity. Clear differences, however, were observed between the Y407E and the double mutant control in the vicinity of the glycan chain and the CH2–CH3 interface (peptides 235–241, 242–252, 300–306). These structural changes are not caused by the antibody populating a monomeric (HL) state, but rather are directly correlated with the enhanced glycosylation induced by the Y407E mutation.

The effect of Y407E mutation on Fc-receptor binding. To determine whether these conformational changes affected Fc-receptor binding properties, the binding of three Y407E constructs (natural mixture, purified dimer and purified monomer) and wild-type IgG1 to FcγRI and mmFcRn were measured by ELISA (**Fig. S11**). The monomer content of Y407E caused a decrease in the binding strength; however, purification of the covalently-bound dimer restored this to wild-type levels. The Y407 to E substitution itself thus does not negatively affect binding of Fc receptors. It is worth noting that the poor ability of monomeric molecules to bind FcRn will likely also affect the pharmacokinetic properties of IgG1-Y407E. Thus, to exploit any specific properties of the unusual glycosylation observed here, this issue would have to be addressed in formulating a construct appropriate for therapeutic use, for example by purifying the dimer or by another approach.

Discussion

Here, we describe how the mutation of a single residue in the CH3 domain changes assembly, structure and glycosylation of human IgG. Interactions between the CH3 domains of the two heavy chains are known to be extensive[17] and it has been suggested that heavy chain assembly promotes the formation of the hinge disulfide bonds rather than vice versa.[23] Indeed, Ridgeway et al. showed that a population of monomer could be detected when heavy chains with T366, T394, F405 or Y407 mutated with "knobs" or "holes" were expressed in HEK-293S cells,[24] either alone or when co-expressed with a "knob" or "hole" counterpart. The amount of monomer, however, was lower than observed in this study. Based on our work with IgG4 lacking the genetic hinge region (IgG4Δhinge), CH3 mutations that significantly weaken the CH3–CH3 interaction were identified. Introduction of these mutations into full-length IgG1 also resulted in variants that predominantly form 75 kDa monomeric HL molecules (**Table 2** and **Table S1**; **Fig. 3**). These studies indicated that the mutation of Y407, among other residues, prevents dimerization of the IgG1 CH3 domains and subsequent formation of the interchain hinge disulfide bonds, precluding the formation of typical 150 kDa IgG1 (HL)$_2$ molecules.

A small portion of Y407E heavy chain (< 10%) does dimerize and forms covalent interchain hinge disulfide bridges (**Table 2**). HDX-MS analysis of this dimeric species revealed a much more exposed structure at the CH3–CH3 interface compared with wild-type IgG, representative of a weaker CH3–CH3 interaction. The Y407 residue of one CH3 domain directly interacts with the Y407 in the other CH3 domain and as such it represents the only residue in human IgG to interact with "itself." Removing this π-stacking interaction should already destabilize this interface significantly; furthermore, substituting Y407 for a charged residue will additionally introduce a repulsive electrostatic effect. This is reflected in these variants populating the monomeric HL state to a greater extent.

A further effect of mutating Y407 to a charged amino acid or glutamine is a massive change in the nature of the glycan chain length and nature, typified by a high abundance of sialic acid, galactose and triantennary structures.

It has been proposed that limited space constraints in the Fc domain prevent further elongation of the glycans of IgG because the tertiary structure around glycosylation sites can control the processing of glycans.[25] It appears that non-covalent interactions existing between the CH2 domain and the nascent glycan[17-19] can

prevent extensive galactosylation or sialylation, as well as further branching from bi-antennary to tri- or tetra-antennary structures. Indeed, mutation of single CH2 residues directly involved in non-covalent interactions with the N-linked glycan in IgG1 and IgG3, F241 and F243, has been shown to increase galactosylation and sialylation.[16,26] Reducing the non-covalent interactions of the glycan with the protein backbone resulted in increased accessibility to glycosylation enzymes in the Golgi apparatus. Extensive elongation of the N-linked glycosylation of IgG may
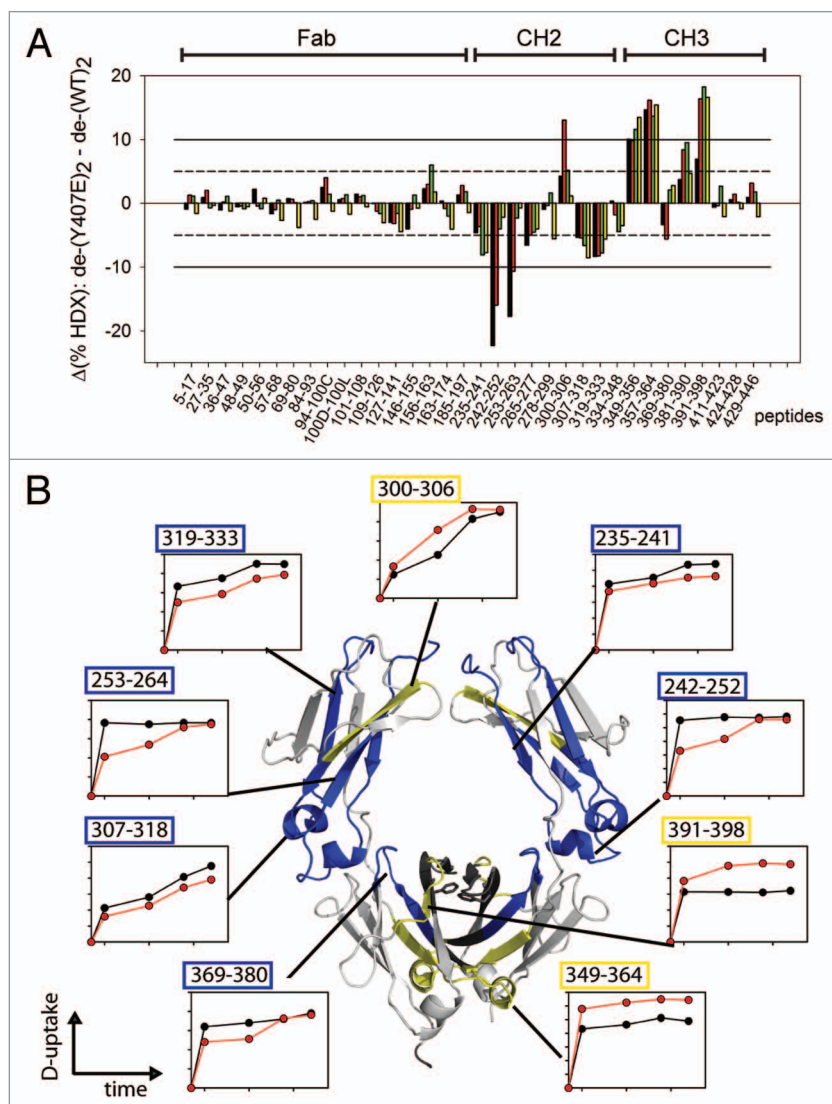
Figure 5. HDX analysis of deglycosylated IgG1-Y407E dimer and wild-type IgG1. (**A**) Difference in HDX for Y407E compared with wild-type at timepoints 1 min (black), 10 min (red), 60 min (green) and 240 min (yellow) for representative peptides spanning the sequence of the heavy chain (N- to C-terminal). No further significant increase in deuterium content was observed after 24 h. (**B**) Peptides with a significant change in % HDX (defined as at least 2 time points showing a difference in deuterium uptake > 5%; average standard deviation of measurements is < 2.5%) are displayed on the crystal structure of an IgG1 Fc (PDB 1hzh). Regions with higher exchange in Y407E are shown in yellow, those with lower exchange in blue. The uptake graphs for each peptide are also indicated (Y407E: red line, wild-type: black line, see **Fig. S8** for more details). The two Y407 residues are shown in stick representation between the CH3 domains.

also be inhibited by the direct pairing of the CH3 domains, as was concluded by Lund et al. after analysis of mutants lacking this entire domain.[27] The highest levels of galactose and sialic acid were observed when the glycosylated CH2 domain was expressed separately, free from association with other domain structures.[27] This work suggested that the IgG architecture, and the presence of paired CH3 domains in particular, have a profound effect on the galactosylation and sialylation of glycans in the CH2.[27] Yet, full galactosylation and subsequent sialylation of glycans in the Fc domain is possible, as intravenous immunoglobulin (IVIG) preparation contains such glycans, although at low amounts.[28] It is also possible to obtain sialylated IgG by enzymatic treatment with galactosyltransferase and sialyltransferase in vitro.[9,12] Therefore it is possible for fully sialylated glycans to reside within the structural constraints of the Fc domain.

We found that monomericity and increased glycosylation are not directly linked, negating the hypothesis that the formation of more complex glycans is limited by the steric influence of the CH3 domains. Furthermore, the distal location of the Y407 residue relative to both the site of glycosylation and the regions known to interact directly with the glycan chain rules out a direct interaction being involved.

Our HDX data revealed changes in the structure, in terms of amide proton exposure, in the CH2 and CH3 domains of IgG1 when Y407 was mutated to glutamine. This was apparent in both enzymatically deglycosylated and glycosylated IgG, suggesting an inherent difference in this protein structure even in the absence of the glycan in both monomeric and dimeric states. Helix 1 in the CH2 domain (residues 247–251) and the B-C loop in the CH3 domain (residues 373–377) were seen to be similarly protected against deuterium incorporation upon Y407 to E mutation (in peptides 245–255 and 369–380). We hypothesize that these changes could be due to a movement of the CH3 domain relative to the CH2 domain, with the CH2–CH3 linker acting as a hinge, bringing the CH2 and CH3 domains closer together or altering the angle between them. This could transmit structural changes into the CH2 domain, and could affect interactions between the nascent glycan chain and the protein, and potentially also the glycosylation enzymes. Peptides containing the residues F241, F243, V264 and R301, for example, have changed structure in Y407E; each of these residues is known to contact the glycan.[29] We hypothesize that a similar mechanism would be responsible for the same phenomenon in IgG4 antibodies. Although the exact nature of the structural changes induced by the Y407 mutations cannot be determined from these data, it is clear that they are likely responsible for the observed changes in glycosylation.

This study reveals an interesting new way to modulate the glycosylation of human IgG. It has previously been shown that IgG with higher levels of galactose has an increased ability to induce CDC,[4-6] thus the mutations described here could be of interest in this regard. Certainly, the alteration of the terminal sugar groups may affect effector functions.[30] It is unclear whether IgG with triantennary structures represent any (functional) benefit compared with IgG with bi-antennary glycans; however, the increased level of sialylation, even of tri-antennary structures, is of great interest.

Ravetch and coworkers showed that α(2,6)-sialylated IgG is responsible for the anti-inflammatory properties of intravenous immunoglobulin (IVIG);[9-12] α(2,3)-sialylated IgG, by contrast, did not have anti-inflammatory properties. Instead of binding to FcγRs, α(2,6)-sialylated IgG appears to bind to the lectin receptor DC-SIGN, which subsequently results in enhanced expression of inhibitory Fcγ receptors, such as FcγRIIb, attenuating inflammation.[31] Application of fully α(2,6)-sialylated IgG in the clinic therefore seems attractive, but the portion of sialylated human IgG in IVIG is very low, as is the sialylation of recombinantly produced IgG.[32,33] The observations described in this paper could potentially be used to obtain sialylated recombinant IgG with anti-inflammatory properties for therapeutic development, especially if a production system that adds only α(2,6)-sialic acid is available. Likewise, recombinant IgG with high levels of galactose could be produced, which may result in increased CDC behavior. Evidently, further format optimization to produce samples with optimal covalent dimer content and to achieve a regular PK profile would be required.

In summary, analysis of IgG-Y407 mutants has given us novel insights into the assembly, structure and glycosylation of human IgG and has opened up new directions for the development of new antibody formats with potentially higher efficacy.

Materials and Methods

Transient expression of human IgG. Expression vectors for IgG1, IgG4 and IgG4Δhinge and the generation of mutants thereof has been described previously.[14,34,35] (Mutated) human IgG was expressed transiently in HEK-293F and CHO-S cells (Invitrogen). HEK-293F cells were cultured in FreeStyle™ 293 Expression Medium (Invitrogen). Plasmids were transfected into HEK-293F cells using 293fectin™ (Invitrogen) as described.[35] FreeStyle™ CHO-S cells (Invitrogen) were transiently transfected using the Freestyle™ Max transfection reagent (Invitrogen), according to the instructions of the manufacturer. All IgG4Δhinge samples used were expressed in HEK-293F cells. Samples were purified as described.[36]

Quantitation of human IgG concentration. Concentrations of human IgG in supernatant were determined using a BNII Nephelometer (Dade Behring) and human serum IgG as a reference. Concentration of purified human IgG was determined by measuring the absorbance at 280 nm using an extinction coefficient of 1.43 AU/mg antibody at a 10 mm path length.

Non-reduced SDS-PAGE analysis. Reducing and non-reducing SDS-PAGE was performed on 4–12% NuPAGE Bis-Tris SDS-PAGE gels (Invitrogen) according to the manufacturer's instructions. Gels were stained with CBB and digitally imaged using the GeneGenius Imaging System (Synoptics).

HP-SEC analysis of human IgG. Batches were analyzed for the presence of monomers, dimers, multimers (molecules larger than 350 kDa) and degraded fragments by high-performance size exclusion chromatography (HP-SEC). The analysis was performed on a Waters Alliance 2695 separation unit (Waters) connected to a TSK G3000SWxl column (Toso Biosciences) and a

Waters 2487 dual λ absorbance detector (Waters). Proteins were detected by measuring the absorbance at 280 nm.

Fractionation of IgG-Y407E. Twenty-eight mg of purified IgG-Y407E produced in CHO-S or HEK-293F was applied to a XK 50/66 column packed with Superdex 200PG (column size of 2.5 × 66 cm) equilibrated in PBS. The column was eluted at a flow rate of 8.0 ml/min. Fractions were analyzed by non-reduced SDS-PAGE and fractions containing 150 kDa dimer or 75 kDa monomer were pooled. The pools were applied to a 5 ml HiTrap MabSelect SuRe, equilibrated in PBS and eluted at a flow rate of 5.0 ml/min. Eluted fractions were dialyzed to PBS using 3–12 ml Slide-A-Lyzers, concentrated in 20 mL Vivaspins (10 kDa MWCO) and sterile-filtered. The concentration of the final pools was determined by measuring the absorbance at 280 nm.

N-linked glycosylation analysis. Samples were analyzed by MALDI/MS and by HPAEC-PAD as described.[36] The presence of 1,3-linked galactose or 1,6-linked galactose was determined in IgG1-Y407E produced in HEK-293F or CHO-S cells. Permethylated glycans of IgG-Y407E were hydrolyzed in 2 M TFA at 120°C for 2 h and subsequently reduced in sodium borodeuteride. After removal of borate by precipitation, the samples were acetylated using acetic anhydride and purified by extraction into chloroform. The partially methylated alditol acetates were then examined by GC-MS. 3'-sialyl and 6'-sialyl lactose were included for reference and permethylated as described.

HDX-MS experiments of IgG1 and IgG1-Y407E. For analysis of IgG1-Y407E in the dimeric, (HL)$_2$ state, material fractionated by SEC was used. For deglycosylated samples, IgG was incubated at 37°C overnight in the presence of PNGaseF (1 unit PNGaseF per 25 µg IgG); complete deglycosylation was confirmed by mass spectrometry analysis. For HDX analysis, 60 pmol IgG (in PBS, pH 7.4) was diluted 20-fold into D$_2$O for 1 min, 10 min, 1 h, 4 h and 24 h. The reaction was quenched by 2:1 dilution into a 0°C solution of 6 M guanidine-HCl, 300 mM TCEP, with pH adjusted to give a final pH of 2.5. The quenched reaction was immediately injected into a Waters HDX/nanoAcquity system for digestion on an online pepsin column (20°C, flow-rate 50 µL/min⁻¹) followed by separation on a 10 min RP-HPLC gradient and MS analysis on a Waters Xevo QTof G2. The online pepsin column (4 cm) was packed with porcine pepsin immobilized on POROS beads (20 µm). RP-HPLC column used was a Waters C18-BEH, 1.0 × 100 mm, with 1.7 µm particles. Electrospray ionization was achieved with a capillary voltage of 3 kV in conjunction with a cone voltage of 30 V and source temperature of 100°C. Mass calibration was performed with sodium formate clusters up to m/z 2000, giving a mass accuracy < 5 ppm. Non-deuterated IgGs were analyzed in the same way for peptide sequencing, using MS^e data acquisition and data processing with ProteinLynx Global Server 2.5 software. Uptake of deuterium for each peptide was calculated compared with the non-deuterated control samples using Waters DynamX 1.0.0 software.

FcRn ELISA binding assay. Recombinant mouse FcRn (mmFcRn) was produced by transient co-expression of the 6xhis-tagged extracellular domain (aa 1–297) of mouse FcRn and mouse β2-microglobulin in HEK-293F cells, followed by purification using Ni-NTA chromatography (Qiagen) and biotinylation using EZ-Link NHS-PEG4-Biotin (Thermo Scientific). The capability of the IgG1 and IgG1-Y407E to interact with mmFcRn was tested in an ELISA. Streptavidin-coated microtiter plates (Roche Diagnostics) were incubated (1 h, RT) with 5 µg/mL (100 µL/well) of biotinylated mmFcRn, diluted in PBS supplemented with 0.05% (v/v) Tween-20 (PBST) and 0.2% (w/v) BSA. Plates were subsequently washed three times with PBST, and 3-fold diluted (in PBST/0.2% BSA, pH 6.0) wild type IgG1 or IgG1-Y407E was added, and incubated for 1 h at RT. Plates were subsequently washed three times with PBST/0.2% BSA, pH 6.0 and incubated (1 h, RT) with goat-anti-human IgG(Fab'2)-HRP (Jackson ImmunoResearch) diluted in PBST/0.2% BSA, pH 6.0. Bound antibodies were visualized using ABTS substrate (Roche Diagnostics) and absorbance was measured at 405 nm.

FcγRI ELISA binding assay. Recombinant human FcγRI was produced by transient expression of the 6xhis-tagged extracellular domain (aa 1–291) in HEK-293F cells, followed by purification using Ni-NTA chromatography (Qiagen). The capability of the IgG1 and IgG1-Y407E to interact with human FcγRI was tested in an ELISA. 96-well microtiter plates (Greiner) were incubated overnight at 4°C with 2 µg/mL (100 µL/well) of IgG1 or IgG1-Y407E, diluted in PBS (coating efficiencies were tested separately and found to be comparable). Plates were subsequently washed 3 times with PBS supplemented with 0.05% (v/v) Tween-20 (PBST) and incubated (1 h, RT) with 3-fold diluted human FcγRI (diluted in PBST supplemented with 0.2% (w/v) BSA). Next, plates were washed 3 times with PBST/0.2% BSA and incubated (1 h, 4°C) with 1 µg/ml of mouse-anti-polyhistidin (R&D Systems) diluted in PBST/0.2% BSA, followed by washing (3× PBST/0.2% BSA) and incubation (1 h, RT) with Streptavidin-poly-HRP (Sanquin) diluted 1:10,000 in PBST/0.2% BSA. After washing (3× PBST/0.2% BSA), bound human FcγRI was visualized using ABTS substrate (Roche Diagnostics) and absorbance was measured at 405 nm.

Supplemental Material

Supplemental material may be downloaded here: www.landesbioscience.com/journals/mabs/article/23532/

References

1. Arnold JN, Wormald MR, Sim RB, Rudd PM, Dwek RA. The impact of glycosylation on the biological function and structure of human immunoglobulins. Annu Rev Immunol 2007; 25:21-50; PMID:17029568; http://dx.doi.org/10.1146/annurev.immunol.25.022106.141702

2. Elbein AD. The role of N-linked oligosaccharides in glycoprotein function. Trends Biotechnol 1991; 9:346-52; PMID:1367760; http://dx.doi.org/10.1016/0167-7799(91)90117-Z

3. Reichert JM. Marketed therapeutic antibodies compendium. MAbs 2012; 4:413-5; PMID:22531442; http://dx.doi.org/10.4161/mabs.19931

4. Tsuchiya N, Endo T, Matsuta K, Yoshinoya S, Aikawa T, Kosuge E, et al. Effects of galactose depletion from oligosaccharide chains on immunological activities of human IgG. J Rheumatol 1989; 16:285-90; PMID:2498512

5. Wright A, Morrison SL. Effect of C2-associated carbohydrate structure on Ig effector function: studies with chimeric mouse-human IgG1 antibodies in glycosylation mutants of Chinese hamster ovary cells. J Immunol 1998; 160:3393-402; PMID:9531299

6. Hodoniczky J, Zheng YZ, James DC. Control of recombinant monoclonal antibody effector functions by Fc N-glycan remodeling in vitro. Biotechnol Prog 2005; 21:1644-52; PMID:16321047; http://dx.doi.org/10.1021/bp050228w

7. Shields RL, Lai J, Keck R, O'Connell LY, Hong K, Meng YG, et al. Lack of fucose on human IgG1 N-linked oligosaccharide improves binding to human Fcgamma RIII and antibody-dependent cellular toxicity. J Biol Chem 2002; 277:26733-40; PMID:11986321; http://dx.doi.org/10.1074/jbc.M202069200

8. Shinkawa T, Nakamura K, Yamane N, Shoji-Hosaka E, Kanda Y, Sakurada M, et al. The absence of fucose but not the presence of galactose or bisecting N-acetylglucosamine of human IgG1 complex-type oligosaccharides shows the critical role of enhancing antibody-dependent cellular cytotoxicity. J Biol Chem 2003; 278:3466-73; PMID:12427744; http://dx.doi.org/10.1074/jbc.M210665200

9. Anthony RM, Nimmerjahn F, Ashline DJ, Reinhold VN, Paulson JC, Ravetch JV. Recapitulation of IVIG anti-inflammatory activity with a recombinant IgG Fc. Science 2008; 320:373-6; PMID:18420934; http://dx.doi.org/10.1126/science.1154315

10. Anthony RM, Wermeling F, Karlsson MCI, Ravetch JV. Identification of a receptor required for the anti-inflammatory activity of IVIG. Proc Natl Acad Sci U S A 2008; 105:19571-8; PMID:19036920; http://dx.doi.org/10.1073/pnas.0810163105

11. Kaneko Y, Nimmerjahn F, Ravetch JV. Anti-inflammatory activity of immunoglobulin G resulting from Fc sialylation. Science 2006; 313:670-3; PMID:16888140; http://dx.doi.org/10.1126/science.1129594

12. Scallon BJ, Tam SH, McCarthy SG, Cai AN, Raju TS. Higher levels of sialylated Fc glycans in immunoglobulin G molecules can adversely impact functionality. Mol Immunol 2007; 44:1524-34; PMID:17045339; http://dx.doi.org/10.1016/j.molimm.2006.09.005

13. Moore GL, Chen H, Karki S, Lazar GA. Engineered Fc variant antibodies with enhanced ability to recruit complement and mediate effector functions. MAbs 2010; 2:181-9; PMID:20150767; http://dx.doi.org/10.4161/mabs.2.2.11158

14. Rose RJ, Labrijn AF, van den Bremer ETJ, Loverix S, Lasters I, van Berkel PHC, et al. Quantitative analysis of the interaction strength and dynamics of human IgG4 half molecules by native mass spectrometry. Structure 2011; 19:1274-82; PMID:21893287; http://dx.doi.org/10.1016/j.str.2011.06.016

15. van der Neut Kolfschoten M, Schuurman J, Losen M, Bleeker WK, Martínez-Martínez P, Vermeulen E, et al. Anti-inflammatory activity of human IgG4 antibodies by dynamic Fab arm exchange. Science 2007; 317:1554-7; PMID:17872445; http://dx.doi.org/10.1126/science.1144603

16. Lund J, Takahashi N, Pound JD, Goodall M, Jefferis R. Multiple interactions of IgG with its core oligosaccharide can modulate recognition by complement and human Fc gamma receptor I and influence the synthesis of its oligosaccharide chains. J Immunol 1996; 157:4963-9; PMID:8943402

17. Deisenhofer J. Crystallographic refinement and atomic models of a human Fc fragment and its complex with fragment B of protein A from Staphylococcus aureus at 2.9- and 2.8-A resolution. Biochemistry 1981; 20:2361-70; PMID:7236608; http://dx.doi.org/10.1021/bi00512a001

18. Krapp S, Mimura Y, Jefferis R, Huber R, Sondermann P. Structural analysis of human IgG-Fc glycoforms reveals a correlation between glycosylation and structural integrity. J Mol Biol 2003; 325:979-89; PMID:12527303; http://dx.doi.org/10.1016/S0022-2836(02)01250-0

19. Sondermann P, Huber R, Oosthuizen V, Jacob U. The 3.2-A crystal structure of the human IgG1 Fc fragment-Fc gammaRIII complex. Nature 2000; 406:267-73; PMID:10917521; http://dx.doi.org/10.1038/35018508

20. Houde D, Arndt J, Domeier W, Berkowitz S, Engen JR. Characterization of IgG1 conformation and conformational dynamics by hydrogen/deuterium exchange mass spectrometry. Anal Chem 2009; 81:5966; PMID:19606834; http://dx.doi.org/10.1021/ac9009287

21. Houde D, Peng Y, Berkowitz SA, Engen JR. Post-translational modifications differentially affect IgG1 conformation and receptor binding. Mol Cell Proteomics 2010; 9:1716-28; PMID:20103567; http://dx.doi.org/10.1074/mcp.M900540-MCP200

22. Burkitt W, Domann P, O'Connor G. Conformational changes in oxidatively stressed monoclonal antibodies studied by hydrogen exchange mass spectrometry. Protein Sci 2010; 19:826-35; PMID:20162626; http://dx.doi.org/10.1002/pro.362

23. Carter P. Bispecific human IgG by design. J Immunol Methods 2001; 248:7-15; PMID:11223065; http://dx.doi.org/10.1016/S0022-1759(00)00339-2

24. Ridgway JBB, Presta LG, Carter P. 'Knobs-into-holes' engineering of antibody CH3 domains for heavy chain heterodimerization. Protein Eng 1996; 9:617-21; PMID:8844834; http://dx.doi.org/10.1093/protein/9.7.617

25. Rudd PM, Dwek RA. Glycosylation: heterogeneity and the 3D structure of proteins. Crit Rev Biochem Mol Biol 1997; 32:1-100; PMID:9063619; http://dx.doi.org/10.3109/10409239709085144

26. Jassal R, Jenkins N, Charlwood J, Camilleri P, Jefferis R, Lund J. Sialylation of human IgG-Fc carbohydrate by transfected rat alpha2,6-sialyltransferase. Biochem Biophys Res Commun 2001; 286:243-9; PMID:11500028; http://dx.doi.org/10.1006/bbrc.2001.5382

27. Lund J, Takahashi N, Popplewell A, Goodall M, Pound JD, Tyler R, et al. Expression and characterization of truncated forms of humanized L243 IgG1. Architectural features can influence synthesis of its oligosaccharide chains and affect superoxide production triggered through human Fcgamma receptor I. Eur J Biochem 2000; 267:7246-57; PMID:11106438; http://dx.doi.org/10.1046/j.1432-1327.2000.01839.x

28. Stadlmann J, Weber A, Pabst M, Anderle H, Kunert R, Ehrlich HJ, et al. A close look at human IgG sialylation and subclass distribution after lectin fractionation. Proteomics 2009; 9:4143-53; PMID:19688751; http://dx.doi.org/10.1002/pmic.200800931

29. Barb AW, Borgert AJ, Liu M, Barany G, Live D. Intramolecular glycan-protein interactions in glycoproteins. Methods Enzymol 2010; 478:365-88; PMID:20816490; http://dx.doi.org/10.1016/S0076-6879(10)78018-6

30. Raju TS. Terminal sugars of Fc glycans influence antibody effector functions of IgGs. Curr Opin Immunol 2008; 20:471-8; PMID:18606225; http://dx.doi.org/10.1016/j.coi.2008.06.007

31. Anthony RM, Ravetch JV. A novel role for the IgG Fc glycan: the anti-inflammatory activity of sialylated IgG Fcs. J Clin Immunol 2010; 30(Suppl 1):S9-14; PMID:20480216; http://dx.doi.org/10.1007/s10875-010-9405-6

32. Jefferis R. Glycosylation of recombinant antibody therapeutics. Biotechnol Prog 2005; 21:11-6; PMID:15903235; http://dx.doi.org/10.1021/bp040016j

33. Jefferis R. Glycosylation of human IgG antibodies: relevance to therapeutic applications. Biopharm 2002; 14:19-26

34. Labrijn AF, Buijsse AO, van den Bremer ETJ, Verwilligen AYW, Bleeker WK, Thorpe SJ, et al. Therapeutic IgG4 antibodies engage in Fab-arm exchange with endogenous human IgG4 in vivo. Nat Biotechnol 2009; 27:767-71; PMID:19620983; http://dx.doi.org/10.1038/nbt.1553

35. van Berkel PHC, Gerritsen J, van Voskuilen E, Perdok G, Vink T, van de Winkel JGJ, et al. Rapid production of recombinant human IgG With improved ADCC effector function in a transient expression system. Biotechnol Bioeng 2010; 105:350-7; PMID:19739094; http://dx.doi.org/10.1002/bit.22535

36. van Berkel PHC, Gerritsen J, Perdok G, Valbjørn J, Vink T, van de Winkel JGJ, et al. N-linked glycosylation is an important parameter for optimal selection of cell lines producing biopharmaceutical human IgG. Biotechnol Prog 2009; 25:244-51; PMID:19224598; http://dx.doi.org/10.1002/btpr.92